Langmuir
Article
pubs.acs.org/Langmuir

Well-Defined Critical Association Concentration and Rapid Adsorption at the Air/Water Interface of a Short Amphiphilic Polymer, Amphipol A8-35: A Study by Förster Resonance Energy Transfer and Dynamic Surface Tension Measurements

Fabrice Giusti,[†] Jean-Luc Popot,[*,†] and Christophe Tribet[*,‡]

[†]UMR 7099, CNRS/Université Paris-7, Institut de Biologie Physico-Chimique, 13 rue Pierre et Marie Curie, F-75005 Paris, France

[‡]Département de Chimie, Ecole Normale Supérieure, CNRS-ENS-UPMC Paris 06 UMR 8640, 24, rue Lhomond, F-75231 Paris Cedex 05, France

Supporting Information

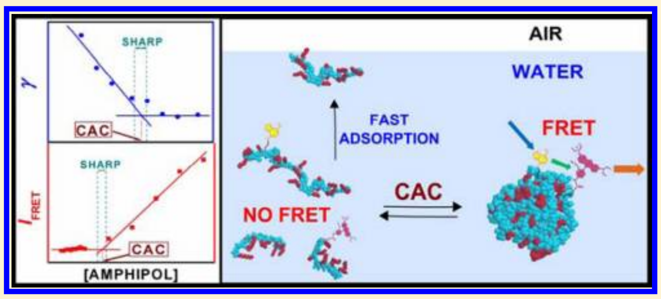

ABSTRACT: Amphipols (APols) are short amphiphilic polymers designed to handle membrane proteins (MPs) in aqueous solutions as an alternative to small surfactants (detergents). APols adsorb onto the transmembrane, hydrophobic surface of MPs, forming small, water-soluble complexes, in which the protein is biochemically stabilized. At variance with MP/detergent complexes, MP/APol ones remain stable even at extreme dilutions. Pure APol solutions self-associate into well-defined micelle-like globules comprising a few APol molecules, a rather unusual behavior for amphiphilic polymers, which typically form ill-defined assemblies. The best characterized APol to date, A8-35, is a random copolymer of acrylic acid, isopropylacrylamide, and octylacrylamide. In the present work, the concentration threshold for self-association of A8-35 in salty buffer (NaCl 100 mM, Tris/HCl 20 mM, pH 8.0) has been studied by Förster resonance energy transfer (FRET) measurements and tensiometry. In a 1:1 mol/mol mixture of APols grafted with either rhodamine or 7-nitro-1,2,3-benzoxadiazole, the FRET signal as a function of A8-35 concentration is essentially zero below a threshold concentration of 0.002 $g \cdot L^{-1}$ and increases linearly with concentration above this threshold. This indicates that assembly takes place in a narrow concentration interval around 0.002 $g \cdot L^{-1}$. Surface tension measurements decreases regularly with concentration until a threshold of ca. 0.004 $g \cdot L^{-1}$, beyond which it reaches a plateau at ca. 30 $mN \cdot m^{-1}$. Within experimental uncertainties, the two techniques thus yield a comparable estimate of the critical self-assembly concentration. The kinetics of variation of the surface tension was analyzed by dynamic surface tension measurements in the time window 10 ms−100 s. The rate of surface tension decrease was similar in solutions of A8-35 and of the anionic surfactant sodium dodecylsulfate when both compounds were at a similar molar concentration of *n*-alkyl moieties. Overall, the solution properties of APol "micelles" (in salty buffer) appear surprisingly similar to those of the micelles formed by small, nonpolymeric surfactants, a feature that was not anticipated owing to the polymeric and polydisperse nature of A8-35. The key to the remarkable stability to dilution of A8-35 globules, likely to include also that of MP/APol complexes, lies accordingly in the low value of the critical self-association concentration as compared to that of small amphiphilic analogues.

INTRODUCTION

Self-association in aqueous solutions is a property shared by many water-soluble polymers containing hydrophobic units.[1−3] Amphiphilic polymers that exhibit such properties generally comprise a combination of hydrophilic units, which keep the polymer water-soluble, and hydrophobic units, which tend to self-assemble. Many types of amphiphilic polymers have been developed. Their hydrophobic side groups are generally *n*-alkyl (typically hexyl to octadecyl) chains. The hydrophilic groups can be zwitterionic (phosphorylcholine[4,5]), neutral (acrylamide,[6] isopropylacrylamide,[7] sugars[8,9]), or anionic (carboxylate[10,11] or sulfonate groups[12,13]). In aqueous solutions, most of these polymers assemble into either micelle-like assemblies,[1,2] vesicles called polymersomes,[14] or transient networks.[15,16] As a rule, the critical self-association concentration (cac) at which interchain associations start to form decreases significantly with increasing amount or density of hydrophobic groups.[11,17] Unsurprisingly, copolymers, especially random ones, tend to form poorly defined aggregates or physical gels containing polymer bridges between several hydrophobic clusters rather than discrete globules. In addition, the degree of association and the equilibrium of globules with unbound chains of amphiphilic polymers tend to evolve above their cac over a much larger concentration range than does that of most

Received: February 23, 2012
Revised: May 3, 2012
Published: June 19, 2012

   dx.doi.org/10.1021/la300774d | *Langmuir* 2012, 28, 10372−10380

small surfactants above their critical micellar concentration (cmc). This is due in part to their polydispersity, both in terms of length and of distribution of hydrophobic groups along the chains.

Polydisperse macroamphiphiles, including random copolymers, can nevertheless be tailored to escape their propensity to aggregation and to form well-defined assemblies in water. Flexible spacers introduced between the polymer backbone and the hydrophobic groups facilitate the formation of well-defined micellar clusters, but long polymers may accommodate several clusters in the same isolated chain.[17] The formation of unimolecular or paucimolecular micelle-like globules is more difficult to achieve. Good examples are short polysoaps, which possess amphiphilic detergent-like repeating units[1] or alternating hydrophilic/hydrophobic units.[18]

We focus here on macromolecules called "amphipols" (APols) (Scheme 1), a class of short-chain homo-, co-, or terpolymers designed as substitutes to the small surfactants (also called detergents) usually employed to handle membrane proteins (MPs) in aqueous solutions.[19] APols have proven useful in a wide range of experimental circumstances, including folding MPs to their native state and synthesizing them in vitro, immobilizing them onto solid supports, and studying them by radiation scattering, light spectroscopy, NMR, or cryoelectron microscopy (reviewed in ref 20). To optimize such applications, a detailed understanding of the solution and adsorption behavior of APols is essential. In particular, optimal amphipols should self-assemble into well-defined globules so as to avoid formation of polydisperse complexes with MPs. A8-35 (Scheme 1), one of the first APols to be developed,[19] remains to date the most extensively used and best characterized one. A8-35 is obtained by random modification of a short poly(acrylate) with octyl and isopropyl side groups.[21−23] The polydispersity of chain lengths of A8-35 and random distribution of their hydrophobic/philic groups do not prevent A8-35 from self-organizing into relatively monodisperse micelle-like globules, whose size and molar mass have been intensively studied. Analytical ultracentrifugation and small angle neutron scattering indicate that the average A8-35 globule has a mass of ∼40 kDa.[22,23] Size exclusion chromatography and dynamic light scattering point to the absence of large aggregates (absence of species of hydrodynamic radius much larger than 5 nm) and a typical average radius of 3.15 nm.[22]

Scheme 1. Schematic Representation of the Synthesis of Fluorescently Labeled APols (FAPols)[a]

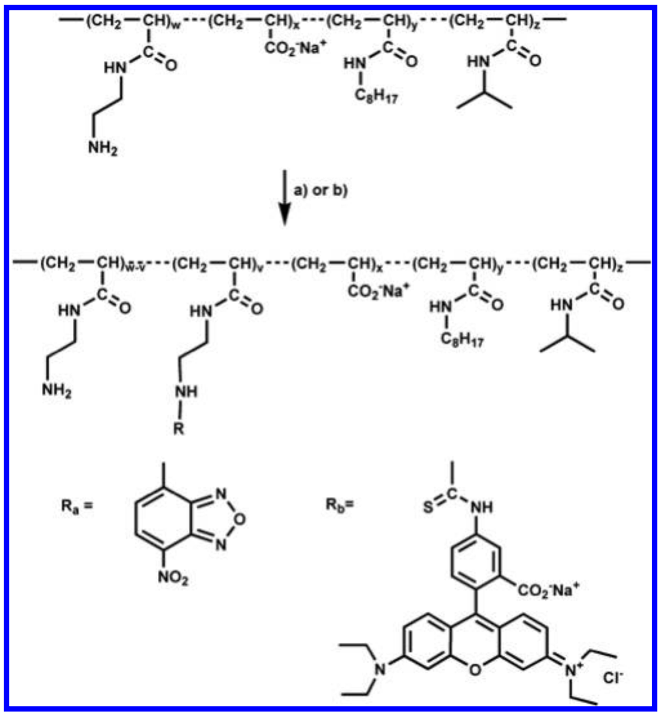

[a]The parent chain is a random poly(acrylic acid) of polydispersity ∼2.5, grafted with octylamine (molar percentage of grafting $y \approx 23\%$), isopropylamine ($z \approx 34\%$), and 2-aminoethylamine ($w \approx 1.5\%$). Experimental conditions: (a) NBD-Cl (4 equiv), MeOH, 40°C, 4 h (see ref 25), yielding $FAPol_{NBD}$ ($R = R_a$, $v \approx 0.5\%$); (b) rhodamine B isothiocyanate (4 equiv), DABCO (cat.), DMF, 40°C, 4 h, yielding $FAPol_{rhod}$ ($R = R_b$, $v \approx 0.3\%$).

In order to detect the transition from individual to assembled APol chains even at very low concentrations, we have resorted to surface tension and fluorescence measurements. Dynamic surface tension measurements were carried out by maximal bubble pressure tensiometry, and equilibrium surface tension was determined in a spinning drop tensiometer in order (i) to estimate the cac and (ii) to collect data on the kinetics of APol adsorption at the air−water interface over a wide time window. The assembly of the chains was investigated by fluorescence spectroscopy (cf. refs 24 and 11). Two fluorescent APols (FAPols) were synthesized by grafting A8-35 with either a donor group (7-nitro-1,2,3-benzoxadiazol-4-yl, NBD), yielding $FAPol_{NBD}$,[25] or an acceptor one (rhodamine), yielding $FAPol_{rhod}$ (present work). The two FAPols were mixed, and the coexistence of the two fluorophores within mixed assemblies was detected by fluorescence quenching and Förster resonance energy transfer (FRET) measurements. The data point to remarkable similarities between the properties of APol assemblies and those of detergent micelles.

■ MATERIALS AND METHODS

Materials. Poly(acrylic acid) (PAA) was from Acros ($M_w \sim 5500$) or Aldrich (M_w 5000). 1,4-Diazabicyclo[2.2.2]octane (DABCO) and rhodamine B were from Acros. *N,N*-Dicyclohexylcarbodiimide (DCI), tris(hydroxymethyl)aminomethane (Tris), sodium chloride (NaCl), and rhodamine B isothiocyanate were from Sigma-Aldrich. Dimethylformamide (DMF) was purchased from SDS (Peypin, France) and used as received. A8-35 (batch FGH29) was prepared and characterized as previously reported.[22] Water ("Milli-Q water") was purified on a Milli-Q system (Millipore, Saint-Quentin-en-Yvelines, France). Except where otherwise specified, Tris buffer was Tris/HCl 20 mM, NaCl 100 mM, pH = 8.0. UV−visible absorption spectra were recorded on an HP 8453 UV−visible spectrophotometer (Agilent Technologies, Massy, France). ^1H and ^{13}C NMR spectra were recorded on a NMR spectrometer (Bruker Avance 400 MHz, Wissembourg, France).

Methods. *Synthesis of FAPols.* $FAPol_{NBD}$ and $FAPol_{rhod}$ were derived from the same precursor, synthesized according to the procedure described in ref 25. Briefly, PAA was modified in *N*-methylpyrrolidone (NMP) in the presence of dicyclohexylcarbodiimide (coupling reagent), first with octylamine and a selectively monoprotected amino linker (*N*-benzoyloxycarbonylethylenediamine) and then with isopropylamine. The three amines were introduced in defined proportions in order to provide the expected A8-35. The linker was deprotected under mild conditions in methanol in the presence of ammonium formate and palladium on activated charcoal and then reacted with 4-chloro-7-nitro-1,2,3-benzoxadiazole (NBD-Cl), yielding $FAPol_{NBD}$ (for a detailed procedure see ref 25). $FAPol_{rhod}$ was obtained by a similar reaction using 4 equiv of rhodamine isothiocyanate in dry DMF in the presence of DABCO (catalytic amount) at 40 °C for 2 h under inert atmosphere. Both FAPols were purified in three steps: (i) by four precipitation cycles in acidic aqueous solution, followed by redissolution at basic pH; (ii) by a 3-day dialysis against Milli-Q water (Spectra/Por dialysis tubing, MWCO = 6−8 kDa); and (iii) by fractionation on a preparative Superose 12 column.[22,25] Fractions were pooled and concentrated to 50 mL under pressure (2 atm) in a Millipore Alphacell stirred cell (VWR). Dialysis and freeze-drying of the resulting solution yielded the purified FAPols in ~50% yield.

Chemical Composition of FAPols. The ratios of grafted amines were estimated by ^1H and ^{13}C NMR (see Supporting Information and refs 23 and 25). The ratio of grafted dye was estimated by UV−visible spectroscopy using as a reference the molar extinction coefficient of molecular analogues of the grafted dye measured in the same buffer. Determination of the amount of rhodamine grafted onto $FAPol_{rhod}$ was based on the extinction coefficient of rhodamine. In water, ε_{555} = 87 000 $L \cdot mol^{-1} \cdot cm^{-1}$ has been published in the case of polymers modified with Rhodamine-ITC.[26] In Tris buffer, we measured ε_{555} = 85 200 $L \cdot mol^{-1} \cdot cm^{-1}$ for free rhodamine B (see Supporting Information). Though both values do not differ by more than experimental uncertainties, we used ε_{555} = 85 200 $L \cdot mol^{-1} \cdot cm^{-1}$, as it was measured under our buffer conditions. For $FAPol_{NBD}$, the extinction coefficient used was that of 3-amino-*N*-(7′-nitrobenz-2′-oxa-1′,3′-diazol-4′-yl)propanoic acid (NBD-alanine), ε_{476} = 24 000 $L \cdot mol^{-1} \cdot cm^{-1}$ (ref 25).

Steady-State Fluorescence Experiments. To study solutions of pure FAPols, the polymers were diluted (from a stock solution at 10 $g \cdot L^{-1}$) in Tris buffer. To study mixtures of $FAPol_{NBD}$ and $FAPol_{rhod}$, a methanolic solution of a 1:1 w/w mixture of the two polymers was prepared and evaporated under reduced pressure and then under vacuum, prior to dissolution in Tris buffer (at 20 $g \cdot L^{-1}$ final concentration of FAPol, i.e., 10 $g \cdot L^{-1}$ of $FAPol_{NBD}$ and 10 $g \cdot L^{-1}$ $FAPol_{rhod}$).

Fluorescence measurements were performed on a PTI fluorescence spectrometer (Serlabo Technologies) using an excitation wavelength of 476 nm and measuring the emission at 575 nm (±1 nm). The day-to-day stability of response of the spectrometer in terms of the output raw intensity (in cps) was checked using reference solutions of each polymer ($FAPol_{NBD}$ or $FAPol_{rhod}$ in Tris buffer at 1, 5, and 10 ppm). Reference solutions were stored in the dark under argon.

Dynamic Surface Tension Measurements. A 10 $g \cdot L^{-1}$ stock solution of A8-35 (FGH29) was prepared at least 24 h in advance and diluted in Tris buffer a few minutes to a few hours prior to measurements on a BPA-1S maximum bubble pressure tensiometer (Sinterface, CAD Instrumentation) equipped with a capillary with an inner diameter of 0.13 mm. The principle of the measurement is described in refs 27−29. In brief, the instrument establishes a stationary regime of air flow and measures the pressure as a function of time. Peaks of maximum pressure are reached when the diameter of the air bubble equals the diameter of the capillary, prior to further bubble growth and detachment. Laplace equation translates this maximum pressure into a value of surface tension that is determined for varying air flows, i.e., at varying bubble life times. The data curves can be analyzed according to models established for small surfactants.[30−32]

Surface Tension Measurements at High Dilutions. Surface tension measurements at high dilution (from 0.1 to 5 × 10^{-4} $g \cdot L^{-1}$) were carried out on a SVT 20 spinning drop video tensiometer (Dataphysics). The principle of measurement and technical details for this tensiometer are reported in refs 33 and 34. Measurements were performed in a borosilicated glass capillary with an inner diameter of 2.45 mm, filled with the buffer or A8-35 solutions. The capillary was plugged, with a bubble of air present on its top, and fixed in the thermostated chamber to be subjected to an axial rotation at rotation speed ranging from 2000 to 7000 rpm. The bubble deformation under the centrifuge force was recorded by a CDD camera and analyzed according to numerical resolution of Young−Laplace equations (ref 35 and refs therein). It was checked that the rotation speed did not affect the measured surface tension by more than the experimental error (0.5 $mN \cdot m^{-1}$). After extensive precleansing of the capillary using chloroform and water, a calibration was carried out by three measurements on Milli-Q water, assuming that records of invariant tension for 30 min were indicative of stable values of 72 $mN \cdot m^{-1}$.

■ RESULTS

Synthesis and Characterization of FAPols. FAPols were synthesized by grafting a fluorophore onto an aminated precursor whose structure and synthesis are described in ref 25 under the name of UAPol. UAPol is a copolymer containing, in molar percentages, ~41.5% free acrylate, ~23% *N-n*-octylacrylamide, ~34% *N*-isopropylacrylamide, and ~1.5% *N*-(2-aminoethyl)acrylamide (Scheme 1). The amino group was allowed to react with a 4-fold molar excess of either NBD chloride or rhodamine isothiocyanate (see Scheme 1) in methanol or DMF, respectively (see Materials and Methods). As described in ref 25, an excess of fluorophore is required because of the weak reactivity of the few amino groups carried by the APol chain. The end product is a mixture of labeled and unlabeled A8-35 and unreacted fluorophore. The polymers were purified by four cycles of precipitation in acidified water (cf. Materials and Methods), followed by a 3-day dialysis and, finally, low-pressure SEC on a Superose 12 preparative column, so as to extensively remove low molecular weight contaminants, especially ungrafted fluorophores. The absence of free fluorophore was evidenced by the presence of a single peak in analytical SEC, detected at the wavelength of maximum visible absorption of the fluorophore. Both FAPols eluted at V_e = 12.1 mL, corresponding to $R_H \approx 3$ nm (Figure 1), which is typical of A8-35.[22] The sharp elution peaks of $FAPol_{NBD}$ and $FAPol_{rhod}$ indeed overlapped exactly that of a standard A8-35 (y = 27%, z = 43%, and w = 0 in Scheme 1), carrying no fluorophore (cf. ref 25).

The presence of a fluorophore therefore does not affect the size of A8-35 globules, a result to be expected as long as the

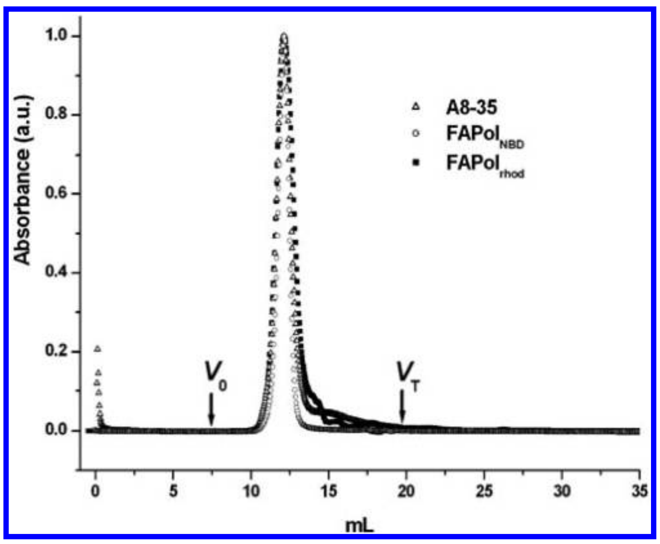

Figure 1. Size exclusion chromatograms of plain and fluorescently labeled amphipols. A8-35 (Δ), $FAPol_{NBD}$ (○), and $FAPol_{rhod}$ (■) were analyzed in Tris buffer (NaCl 100 mM, Tris/HCl 20 mM, pH 8.0) using an Äkta Purifier 10 system equipped with a Superose 12 10-300 GL column. Detection was by absorbance at 220 ± 2 nm (A8-35), 340 nm ($FAPol_{NBD}$), or 560 nm ($FAPol_{rhod}$). The chromatograms have been normalized to the same maximum. V_0 and V_T are the excluded and total volumes, respectively.

extent of grafting is kept low. Here, a grafting molar fraction of 0.5% has been achieved for $FAPol_{NBD}$ and 0.3% for $FAPol_{rhod}$. As a consequence, 40-kDa self-assembled globules of $FAPol_{NBD}$ are expected to contain on average ~1.62 NBD groups, whereas those of $FAPol_{rhod}$ would contain ~0.97 rhodamine groups. Of importance to studying the self-assembly of the chains by FRET, the presence of a small number of fluorophores per particle implies that mixed FAPol assemblies contain predominantly zero or one rhodamine and zero or one NBD group. More precisely, Poisson's distribution indicates that in assemblies made of $FAPol_{NBD}$ and $FAPol_{rhod}$ in 1:1 ratio, ~61.5% of the micelles are devoid of rhodamine, ~29.9% contain a single one, and ~7.3% contain two. Similarly, ~44.4% of the mixed assemblies are expected to contain no NBD moiety, ~36% to contain one, and ~14.6% two. Statistically, this means that ~21.4% of the mixed assemblies are expected to contain at least one copy of each fluorophore and to be susceptible to experience FRET.

Determination of the Cac of A8-35 by Steady-State Fluorescence Measurements. The spectral properties of pure FAPols are reported in Figure 2A–C. $FAPol_{NBD}$, upon being excited at 476 nm, shows a broad emission peak (Figure 2A) that overlaps with the excitation spectrum of $FAPol_{rhod}$ (Figure 2C). The estimated Förster distance between the two fluorophores lies between the radius and the diameter of APol globules (see Supporting Information, Table SI.1), making FRET between the two FAPols possible. In 1:1 mixtures of the two FAPols, FRET is evidenced by an enhanced emission by rhodamine and a drop of emission by NBD as compared to the spectrum expected from the addition of the emission spectra of the two pure FAPols (Figure 2D). For cac determination, the fluorescence intensity was measured at 575 nm, i.e., close to the emission maximum of $FAPol_{rhod}$, upon excitation at 476 nm, which is optimal for $FAPol_{NBD}$. Under these conditions, an excellent proportionality between APol concentration and fluorescence intensity is observed in solutions containing only one of the two FAPols (Supporting Information, Figure SI.1). Emission coefficients, defined as the ratio of emission intensity (in counts per second, "cps") to polymer concentration, namely $\alpha_{NBD} = 3.38 \times 10^7$ cps·g^{-1}·L (±4%) and $\alpha_{rhod} = 2.40 \times 10^7$ cps·g^{-1}·L (±4%), were determined for each FAPol in Tris buffer. The linear dependence of fluorescence intensity on concentration indicates that any internal filter effect is negligible. Using the absorbance of samples at their highest final concentration of 0.01 g·L^{-1} (of each FAPol), it can indeed be calculated that in 1:1 mixtures the correction of fluorescence intensity for internal filter effect should be <2.5% of the total intensity.

The experimental emission intensity, I_{exp} (=measured intensity corrected from fluorescence of Tris buffer), was compared to that expected from a linear addition of the contributions of the two FAPols (Figure 3A). The excess emission, I_{FRET}, observed at 575 nm for 1:1 mixtures, is defined as

$$I_{FRET} = I_{exp} - C_{pol}(\alpha_{NBD} + \alpha_{rhod})/2 \quad (1)$$

with C_{pol} = [$FAPol_{NBD}$] + [$FAPol_{rhod}$]. As shown in Figure 3B, an initial plateau where $I_{FRET} \approx 0$ turns, above a given concentration threshold, into a linear increase of I_{FRET} with

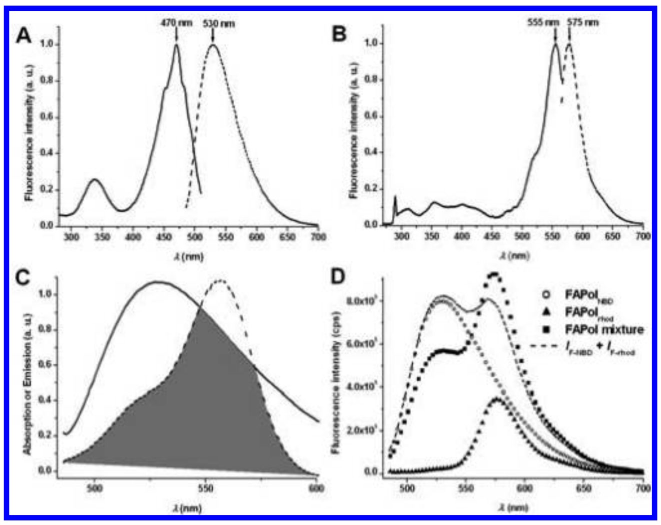

Figure 2. Fluorescence properties of $FAPol_{NBD}$, $FAPol_{rhod}$, and their 1:1 mixture in Tris buffer. (A) FAPolNBD excitation (—) and emission (---) spectra. The maxima of excitation and emission were observed at 470 and 530 nm, respectively. (B) $FAPol_{rhod}$ excitation (—) and emission (---) spectra. The maxima of excitation and emission were observed at 555 and 575 nm, respectively. The four spectra have been normalized to the same maximum. (C) $FAPol_{rhod}$ absorption spectrum (---) superimposed onto the emission spectrum of $FAPol_{NBD}$ (—). The two spectra have been normalized to the same maximum. The spectral overlap is indicated in gray. (D) Fluorescence emission spectra of $FAPol_{NBD}$ (○), $FAPol_{rhod}$ (▲), and a 1:1 w/w mixture of the two FAPols (■) upon excitation at 476 nm (the concentration of each polymer was 0.01 g·L^{-1}); (---) spectrum obtained by addition of the spectra of the two FAPols, i.e., the emission spectrum expected from a solution containing 0.01 g·L^{-1} $FAPol_{NBD}$ and 0.01 g·L^{-1} $FAPol_{rhod}$ in the absence of energy transfer.

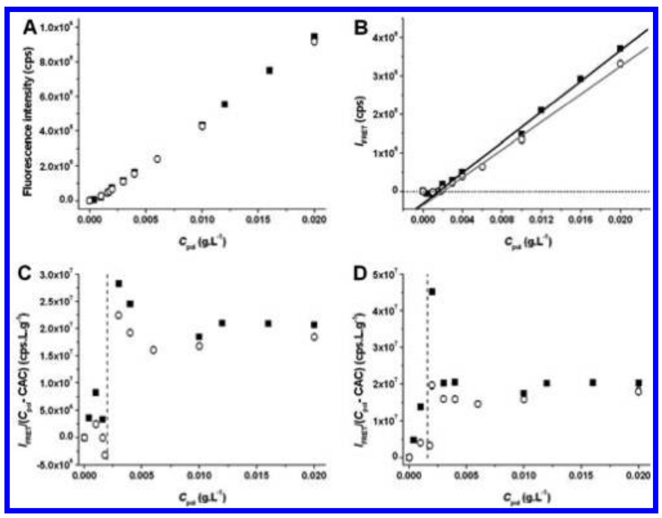

Figure 3. Intensity of fluorescence (λ_{exc} = 476 nm, λ_{em} = 575 nm) of a 1:1 w/w mixture of $FAPol_{NBD}$ and $FAPol_{rhod}$ in Tris buffer (pH = 8) as a function of total polymer concentration C_{pol} = [$FAPol_{NBD}$] + [$FAPol_{rhod}$]. (A) Two independent experiments performed under the same conditions using samples prepared independently are noted by symbols ■ and ○. (B) I_{FRET} (λ_{exc} = 476 nm, λ_{em} = 575 nm) calculated from eq 1 and plotted against C_{pol}. The straight lines extrapolate to I_{FRET} = 0 for C_{pol} = 0.0018 ± 0.0004 and 0.002 ± 0.0002 g·L^{-1}. (C) $I_{FRET}^* = I_{FRET}/(C_{pol} - \text{cac})$ plotted against C_{pol}, using cac = 0.002 g·L^{-1} (vertical dashed line), the average of the two values obtained by extrapolating to I_{FRET} = 0, the two straight lines in B. (D) Same as panel C, but using a cac value of 0.0016 g·L^{-1} (within experimental error of the cac value obtained by extrapolation of the data in B).

increasing C_{pol}. Figure 3B shows two sets of data obtained from independent preparations made at two different periods of time for the sake of testing the reproducibility of measurements. Extrapolating the two straight lines in Figure 3B to $I_{FRET} = 0$ and averaging the two concentrations thus obtained yield an estimate of the concentration threshold of ~0.002 g·L^{-1}. Below this concentration, the excitation of FAPol$_{NBD}$ is essentially not transferred to rhodamine. Above it, a roughly constant fraction of the excitation is transferred, as shown in the plot of $I_{FRET}/(C_{pol} - \text{cac})$ vs C_{pol} in Figure 3C. This abrupt transition in fluorescence properties betrays the existence of a critical concentration of mixed aggregation between FAPol$_{rhod}$ and FAPol$_{NBD}$ around 0.002 g·L^{-1}. The plateau at high concentration and the abrupt jump of $I_{FRET}/(C_{pol} - \text{cac})$ are robust within experimental uncertainties, as shown in Figure 3D, where the cac has been assumed to be 0.0016 g·L^{-1}. A cac of 0.002 g·L^{-1} corresponds to ~4 μM octyl groups. The plateau of $I_{FRET}/(C_{pol} - \text{cac})$ indicates that the extent of FRET per mass of APol particles is constant. This implies that the number of chains per APol globule does not depend on the concentration of polymer, consistent with DLS and SANS measurements carried out at much higher concentrations.[22]

Estimation of the Cac by Surface Tension Measurements. The equilibrium surface tension of A8-35 solutions was determined by extrapolating to long times the variation of surface tension measured in a spinning drop tensiometer. One advantage of this method is the absence of contact between the air bubble and solid surfaces, which limits perturbations by contaminants, especially at high dilutions. As typically observed in the presence of amphiphiles, the surface tension of A8-35 solutions drops at a rate that slows down upon approaching equilibrium (Figure 4A). For small amphiphiles, the rate of variation of the surface tension at long incubation times usually decreases in proportion to the reciprocal square root of time (cf. refs 31 and 32):

$$\gamma(t)_{t\to\infty} = \gamma_{eq} + \frac{\nu RT\Gamma^2}{2C}\sqrt{\frac{\pi}{2Dt}} \qquad (2)$$

with γ_{eq} being the surface tension at equilibrium, RT Boltzmann's term, D the diffusion coefficient of the amphiphile, C the concentration of amphiphile in bulk, Γ the specific surface area per amphiphile at saturation, and ν equal to 1 (neutral amphiphile) or 2 (adsorption of a dissociated 1:1 simple salt). Figure 4B shows representative examples of extrapolating $\gamma(t)$ vs $t^{-1/2}$ by linear regression to obtain the γ_{eq} values shown in Figure 4C. At concentrations above 0.01 g·L^{-1}, γ_{eq} reaches a plateau of 31 ± 1 mN·m^{-1}. At concentrations below ~0.002 g·L^{-1}, γ_{eq} decreases monotonously with increasing APol concentration (Figure 4C). In the case of monomeric surfactants, the crossover between these two regimes conventionally identifies, in a semilogarithmic plot, the threshold concentration at which self-assembly occurs. Given the experimental uncertainties involved in extrapolating γ to an "infinite" equilibration time, as well as to the possible contribution of contaminants, we estimate here a threshold concentration window of 0.004–0.008 g·L^{-1} (Figure 4C). According to surface tension measurements, self-assembly therefore occurs slightly above the concentration of ~0.002 g·L^{-1} determined by FRET. Note that the time axis in Figure 4 assumes a somewhat arbitrary delay of 100 s between the preparation of the air bubble and the first measurement. In practice, extrapolations were applied in the time window between 500 and 3000 s, and it was checked that arbitrary delays chosen between 50 and 200 s affect γ_{eq} by less than 0.3 mN·m^{-1}, i.e., less than the experimental uncertainty.

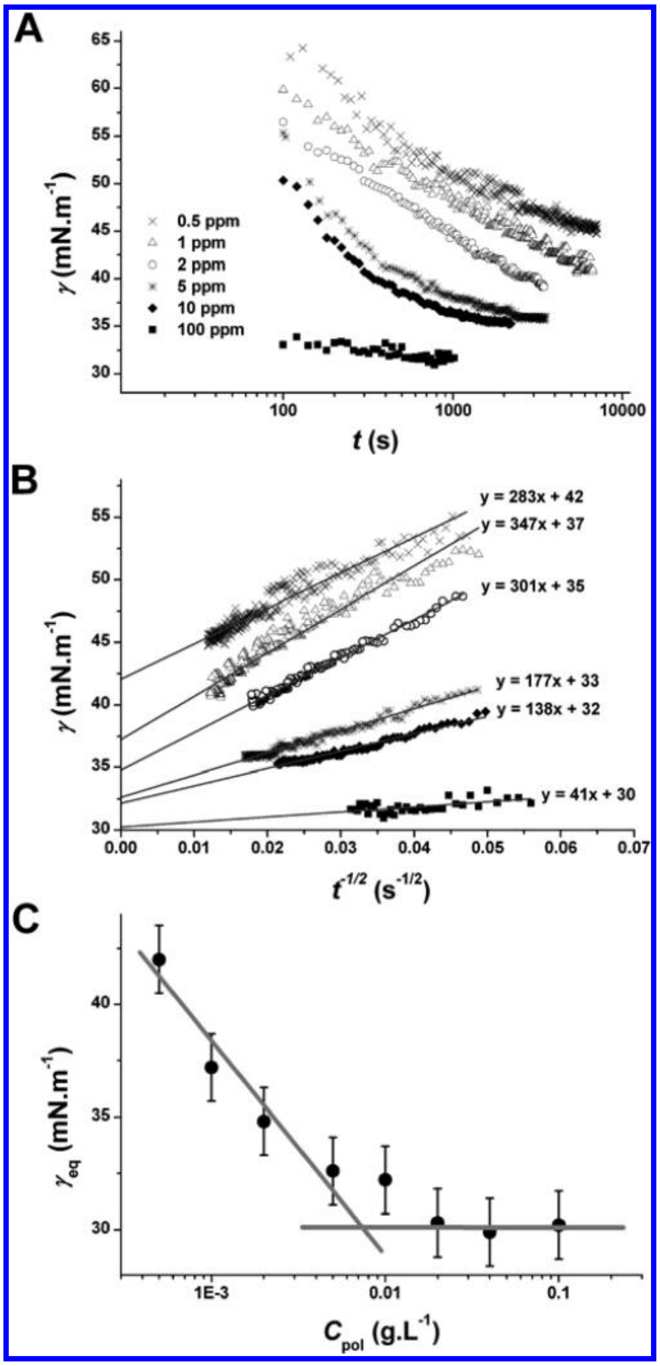

Figure 4. Surface tension of A8-35 solutions in Tris buffer, measured by spinning drop tensionmetry, as a function of incubation time. (A) Evolution of γ as a function of the bubble lifetime. A8-35 concentrations, in g·L^{-1}, were 5×10^{-4} (×), 10^{-3} (Δ), 2×10^{-3} (○), 5×10^{-3} (*), 10^{-2} (◆), and 0.1 (■). (B) Plot of γ vs $t^{-1/2}$ and linear regression (solid lines and equations) extrapolating the surface tension at long times. (C) Variation of the equilibrium surface tension γ_{eq} with APol concentration as determined by extrapolation at infinite time, as shown in panel B (for the sake of clarity some data points have been omitted in panels A and B). Lines are guides for the eye.

Adsorption Rate of A8-35 at the Air–Water Interface. Dynamic surface tension (DST) measurements using the maximum pressure bubble method provide information about the kinetics of adsorption at the air−water interface. In Figure 5, the rate of adsorption of A8-35, examined over two decades

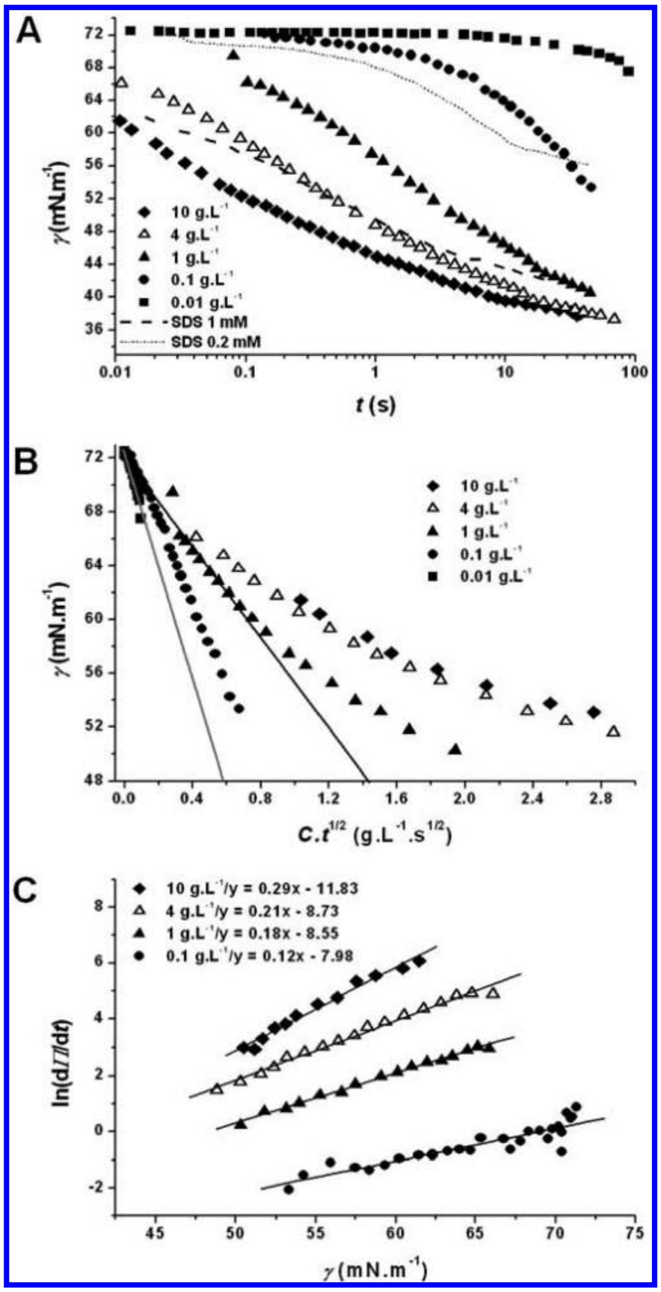

Figure 5. Dynamic surface tension of A8-35 solutions in Tris buffer, measured by the maximum bubble pressure method. APol concentrations: 0.01 $g \cdot L^{-1}$ (■), 0.1 $g \cdot L^{-1}$ (●), 1 $g \cdot L^{-1}$ (▲), 4 $g \cdot L^{-1}$ (△), 10 $g \cdot L^{-1}$ (◆). (A) Plot of γ vs time. Dotted and dashed lines are for solutions of sodium dodecyl sulfate in 100 mM NaCl, at 0.2 and 1 mM, respectively (N.B., 1 $g \cdot L^{-1}$ A8-35 corresponds to a concentration of octyl moieties of ∼2 mM). (B, C) Plot of the same data under the forms suggested by eqs 3 (B) or 4 (C), with the same symbols as in A. Linear regression parameters are indicated.

of APol concentrations, is seen to decrease markedly with decreasing polymer concentration. In the absence of a kinetic barrier against adsorption, which is a reasonable expectation at low surface coverage, i.e., at high surface tension, the rate of adsorption should be diffusion controlled and, for small surfactants, it is expected that the surface tension varies as the square root of time

$$\gamma(t)_{t\to\infty} = \gamma_0 - 2RTC\sqrt{\frac{Dt}{\pi}} \tag{3}$$

with the same definition of parameters as in eq 2. For A8-35 solutions, plots of γ vs $Ct^{1/2}$ (Figure 5B) display a linear decrease at short times, as expected for this purely diffusive model. The initial (negative) slope increases however by a factor of ∼2 with increasing C over two decades, i.e., the "effective" diffusion coefficient D seems to decrease upon increasing the polymer concentration. This deviation from eq 3, which would predict at constant D the same slope irrespective of C, betrays that a repulsion barrier against adsorption gradually develops with increasing concentrations, including at low surface coverage. In addition, experimental data deviate from the linearity predicted by eq 3 as soon as γ decreases below ∼65 $mN \cdot m^{-1}$, which also points to repulsive steric and Coulombic interactions between polymers in solution and the adsorbed layer.

An analysis of the kinetics of variation of surface tension at short times (Figure 5) provides some insight into the origin of the adsorption barrier. It shows, first, that the slow processes evidenced in layers of long polymers are not relevant here to describe APol adsorption. Toomey[36] and Millet[37] analyzed experimental data of variations of the adsorbed amount of amphiphilic chains that were almost linear vs log(t), at long times, which is not the case of A8-35. More satisfactory predictions can be derived from by assuming that the kinetics of adsorption is essentially determined by short-range repulsion. To describe this process, it is assumed that an energy barrier builds up due to the compression of the interfacial layer against the surface pressure, $\Pi = \gamma_0 - \gamma$, as required to create an area ΔA_1 to make room for a new particle.[38] The adsorption rate is then given by

$$\ln(\mathrm{d}n/\mathrm{d}t) = \ln(b) - \frac{\Pi \Delta A_1}{kT} \tag{4}$$

where n is the surface excess, and b a constant parameter that includes kinetics prefactors (including the subsurface concentration). In the limit of low surface coverage, the surface pressure Π varies in proportion to n (i.e., we neglect long-range interactions between adsorbed particles). Accordingly, when the adsorption rate is limited by the adsorption barrier, the plot of $\ln(\mathrm{d}\Pi/\mathrm{d}t)$ vs γ is expected to approach linearity. Such a model matches experimental data quite well (Figure 5C), yielding an effective area ΔA_1 = 0.8−1.2 nm^2. The small value of ΔA_1, as compared to the size of the A8-35 globule (R_s = 3.15 nm),[22] may indicate that APol is attached to the interface by a fraction of the chain and/or that adsorption significantly affects the shape and/or the aspect ratio of the globules.

The equilibrium surface tension was reached relatively rapidly at the highest APol concentrations. At 4 and 10 $g \cdot L^{-1}$ A8-35, values as low as 35 $mN \cdot m^{-1}$ were reached within 100 s, tending toward γ_{eq} = 31 ± 1 $mN \cdot m^{-1}$. A gauge of the rate of surface tension drops consists of a comparison with SDS solutions in 100 mM NaCl.[32] Dotted and dashed lines in Figure 5A show our measurements under conditions that correspond to standard ones in ref 32. The ionic strength in the conditions used with APols (Tris buffer) is similar to conditions in ref 32 (actually 10% higher due to the presence of Tris and its counterions in addition to NaCl). Interestingly, the rate of decrease of the surface tension is roughly comparable for 0.2 and 1 mM SDS solutions and 0.1 and 4 $g \cdot L^{-1}$ A8-35 solutions, respectively (Figure 5A). Expressed as a molar concentration, 0.1 $g \cdot L^{-1}$ A8-35 corresponds to ~0.2 mM *n*-octyl side chains. At similar concentration of *n*-alkyl moieties in the solution, the surface tension of SDS and APol solutions is thus observed to decrease at comparable rate. This result was not anticipated for two reasons. First, when homologous small surfactants are compared by DST at the same concentration, the longer their alkyl chain length, the faster the drop of surface tension,[39] which should favor a more rapid decrease of surface tension with SDS than with A8-35. Second, slow kinetics of adsorption and long equilibration time of the surface tension are typically reported for conventional amphiphilic polymers,[40,41] as compared to small surfactants, which would have the opposite effect. Whatever the underlying mechanism, we observe that A8-35 in Tris buffer adsorbs at the air/water interface more rapidly than is usually found for polymers, which is consistent with the rapid equilibration of APol assemblies observed in solution.[25]

■ DISCUSSION

In many studies of short, highly hydrophobic copolymers, and especially of APols, their self-assembly features clear similarities with the micellization of small surfactants. We do not evoke here assemblies of diblock polymers, whose blocky structure is obviously well adapted to segregation of the hydrophobic and hydrophilic domains in the final assemblies. In contrast, the structure of random copolymers does not necessarily match the constraints imposed by the hydrophobic collapse into micelle-like particles, suggesting that one should expect defects in micellar structures and deviation from micelle-like behavior. It has been proposed that amphiphilic polymers with optimal chain length and optimal hydrophobicity may form unimolecular micelles.[10] Experimental investigation, however, revealed that most polymers tend to form ill-defined aggregates (which may coexist with small micelles).[10,12] In addition, because of their deviations from simple micellization schemes, most amphiphilic copolymers self-assemble over a broad range of concentrations and, therefore, have an ill-defined cac.[11,42] It seems however that, for A8-35 and other APols, which are characterized by a short polymer length (<100 monomers) and a fraction of hydrophobic moieties ≥25%, an optimum structure/composition of the chains has been reached, which can force self-assembly into globules containing a few macromolecules. A8-35 globules comprise ~80 octyl chains,[22] as do octylglucoside micelles.[43] These assemblies present a sharp interface with water (see SANS studies in refs 22 and 18 and MD simulations in ref 44), and their size does not markedly depend on polymer length.[45,9a] In the same way as exchanges occur between conventional micelles of surfactants and the water phase, amphiphilic polymers exchange between water and self-assembled particles[46,5] in a dynamic, non-cooperative manner. Like small surfactants, amphiphilic polymers adsorb at the air–water interface and onto hydrophobic interfaces, reducing the surface tension of water down to 30–40 $mN \cdot m^{-1}$ (refs 9a, 41, 47, and present work)

The self-assembly of A8-35 into small, well-defined globules[22] suggested that this polymer may have a well-defined cac. Previous investigations of aqueous solutions of APol A8-35 and other APols by SANS, DLS, and ITC[5,22] failed to detect particle dissociation down to 0.1 $g \cdot L^{-1}$ polymer (in NaCl 100 mM, Tris/HCl 20 mM, pH 7.8), so that no conclusion could be drawn. The present study shows that A8-35 has a very low cac, ~0.002 $g \cdot L^{-1}$. In comparison, the cmc of usual neutral detergents whose hydrophobic tails typically contain 8–12 carbon atoms (such as octylglucoside, dodecylmaltoside, etc.) is >0.1 mM, which expressed as a mass concentration correspond to cmc > 0.05 $g \cdot L^{-1}$.

Finally, the present results reveal, surprisingly, that the kinetics of adsorption of APol particles to the air–water interface is as rapid as that of SDS. In contrast, slow processes (days long) have been reported for the effect of amphiphilic polymers on lipid membranes, such as the day-long solubilization of lipids into mixed particles.[48,49] A marked slowing down over time and deviations from diffusive behavior have been reported for most cases of polymer adsorption, including that of micelle-forming diblock copolymers[36] and that of A8-35 analogs with longer main chains.[37] Even the equilibrium nature of the adsorption is questioned for long-chain[50] and multiblock[51] copolymers at the air–water interface. In the case of A8-35, Coulombic and steric repulsions may be lowered by (i) the relatively high ionic strength used in the present study and (ii) the lack of coiled conformations or long loops protruding aways from the polymer micellar globule,[22,44] which diminishes the range of steric repulsion. Accordingly, APol A8-35 decreases the surface tension, i.e., covers the interface, at a rate that is comparable to that observed with detergents such as SDS at similar concentrations of alkyl moieties. Above a concentration of 0·1 $g \cdot L^{-1}$, the process is essentially over in less than 2 min.

From the biochemist's points of view, the present data clarify some issues concerning the use of APol A8-35 to stabilize MPs. First, the low cac implies that, under most usual circumstances, where the total concentration of APol typically ranges between 0.1 and 10 $g \cdot L^{-1}$, most of the polymer present in the preparations will be either adsorbed onto the MP under study or assembled into ~40-kDa particles. It will not, for instance, dialyze across standard membranes, whose MW cutoff is ~12 kDa. Dilution of MP/A8-35 preparations to such an extent that the concentration of A8-35 will fall below its cac rarely happens. Practically, conditions of extensive removal of free APol are reached when immobilized MPs, for instance MPs attached to avidin-carrying beads or chips via a biotinylated version of A8-35, are washed with detergent-free buffer.[52] In the latter case, surface plasmon resonance and fluorescence experiments show that MPs remain attached and in their native state. This result suggests that most MP/A8-35 complexes may persist and stabilize MPs even well under the cac of A8-35.

■ CONCLUSIONS

This study by fluorescence and surface tension measurements has shown that the random, anionic, amphiphilic polymer A8-35 self-assembles above a threshold concentration and reaches equilibrium interfacial coverage as rapidly as sodium dodecyl sulfate. Despite the polydisperse nature of APols and a possible role of steric constraints hampering the assembly of polymers in water, the formation of paucimolecular globules resembles the micellization of small surfactants with respect to the existence of a critical assembly concentration and the well-defined size of the particles. This behavior was not anticipated given the classically ill-defined aggregation concentration of usual hydrophobic copolymers. The unusual properties of A8-35 probably originate from its peculiar composition (high density of hydrophobic groups, short chains), which may minimize the defects occurring upon gathering covalently linked hydrophobic moieties into a single core. The low cac of A8-35 is of importance with respect to its use to stabilize membrane proteins in aqueous solutions under the form of MP/APol complexes. Indeed, lowering the concentration of free A8-35 below its cac of ~0.002 $g\cdot L^{-1}$ is not commonly achieved under usual experimental conditions. APols appear, from this point of view, as an excellent compromise between lipids and detergents: they keep MPs soluble by covering their transmembrane region with an amphipathic layer that rapidly reaches equilibration, thereby mimicking labile micelles, but at the same time they form, under an extended range of conditions, stable assemblies that, like lipid vesicles, do not vanish upon dilution.

■ ASSOCIATED CONTENT

Supporting Information

NMR spectra of FAPols; derivation of the Förster distance, R_0, in solvents of various dielectric constant; variation of fluorescence intensity with polymer concentration in solutions of each FAPol; and determination of the extinction coefficient of rhodamine B. This information is available free of charge via the Internet at http://pubs.acs.org/.

■ AUTHOR INFORMATION

Corresponding Author

*E-mail: christophe.tribet@ens.fr (C.T.); jean-luc.popot@ibpc.fr (J.-L.P.).

Notes

The authors declare no competing financial interest.

■ ACKNOWLEDGMENTS

The authors would like to thank Milena Opačić (UMR7099) for useful discussions and advice about fluorescence spectroscopy. This work was supported by the CNRS, by University Paris-7, and by grants from the E.U. (Specific Targeted Research Project LSHGCT-2005-513770 IMPS: Innovative tools for membrane protein structural proteomics) and from the French Ministry of Research (ANR-06-BLAN-0087, ANR-2010-INTB-1501).

■ REFERENCES

(1) Laschewsky, A. Molecular concepts, self-organisation and properties of polysoaps. *Adv. Pol. Sci., Polysoaps/Stabilizers/Nitrogen-15 NMR* **1995**, *124*, 1−86.

(2) Borisov, O. V.; Halperin, A. Self-assembly of polysoaps. *Curr. Opin. Colloid Interface Sci.* **1998**, *3* (4), 415−421.

(3) Summers, M.; Eastoe, J. Applications of polymerizable surfactants. *Adv. Colloid Interface Sci.* **2003**, *100*, 137−152.

(4) Miyazawa, K.; Winnik, F. M. Solution properties of phosphorylcholine-based hydrophobically modified polybetaines in water and mixed solvents. *Macromolecules* **2002**, *35* (25), 9536−9544.

(5) Diab, C.; Winnik, F. M.; Tribet, C. Enthalpy of interaction and binding isotherms of non-ionic surfactants onto micellar amphiphilic polymers (amphipols). *Langmuir* **2007**, *23* (6), 3025−3035.

(6) Feng, Y. J.; Billon, L.; Grassl, B.; Bastiat, G.; Borisov, O.; François, J. Hydrophobically associating polyacrylamides and their partially hydrolyzed derivatives prepared by post-modification. 2. Properties of non-hydrolyzed polymers in pure water and brine. *Polymer* **2005**, *46* (22), 9283−9295.

(7) Ringsdorf, H.; Venzmer, J.; Winnik, F. M. Fluorescence studies of hydrophobically modified poly(*N*-isopropylacrylamides). *Macromolecules* **1991**, *24* (7), 1678−1686.

(8) (a) Nishikawa, T.; Akiyoshi, K.; Sunamoto, J. Supramolecular assembly between nanoparticles of hydrophobized polysaccharide and soluble protein complexation between the self-aggregate of cholesterol-bearing pullulan and α-chymotrypsin. *Macromolecules* **1994**, *27*, 7654−7659. (b) Morimoto, N.; Winnik, F. M.; Akiyoshi, K. Botryoidal assembly of cholesteryl-pullulan/poly(*N*-isopropylacrylamide) nanogels. *Langmuir* **2007**, *23* (1), 217−223.

(9) (a) Sharma, S. K.; Durand, G.; Gabel, F.; Bazzacco, P.; Le Bon, C.; Billon-Denis, E.; Catoire, L. J.; Popot, J.-L.; Ebel, C.; Pucci, B. Non-ionic amphiphilic homopolymers: Synthesis, solution properties, and biochemical validation. *Langmuir* **2012**, *28* (10), 4625−4639. (b) Bazzacco, P.; Billon-Denis, E.; Sharma, S. K.; Catoire, L. J.; Mary, S.; Le Bon, C.; Point, E.; Banères, J.-L.; Durand, G.; Zito, F.; Pucci, B.; Popot, J.-L. Non-ionic homopolymeric amphipols: Application to membrane protein folding, cell-free synthesis, and solution NMR. *Biochemistry* **2012**, *51* (7), 1416−1430.

(10) Suwa, M.; Hashidzume, A.; Morishima, Y.; Nakato, T.; Tomida, M. Self-association behavior of hydrophobically modified poly(aspartic acid) in water studied by fluorescence and dynamic light scattering techniques. *Macromolecules* **2000**, *33* (21), 7884−7892.

(11) Petit-Agnely, F.; Iliopoulos, I.; Zana, R. Hydrophobically modified sodium polyacrylates in aqueous solutions: Association mechanism and characterization of the aggregates by fluorescence probing. *Langmuir* **2000**, *16* (25), 9921−9927.

(12) Yamamoto, H.; Morishima, Y. Effect of hydrophobe content on intra- and interpolymer self-associations of hydrophobically modified poly(sodium 2-(acrylamido)-2-methylpropanesulfonate) in water. *Macromolecules* **1999**, *32* (22), 7469−7475.

(13) Dahmane, T.; Giusti, F.; Catoire, L. J.; Popot, J.-L. Sulfonated amphipols: Synthesis, properties and applications. *Biopolymers* **2011**, *95*, 811−823.

(14) Wu, D.; Abezgauz, L.; Danino, D.; Ho, C. C.; Co, C. C. Alternating polymer vesicles. *Soft Matter* **2008**, *4* (5), 1066−1071.

(15) Branham, K. D.; Davis, D. L.; Middleton, J. C.; McCormick, C. L. Water-soluble polymers. 59. Investigation of the effects of polymer microstructure on the associative behavior of amphiphilic terpolymers of acrylamide - acrylic-acid and *N*-(4-decyl)phenyl acrylamide. *Polymer* **1994**, *35* (20), 4429−4436.

(16) Yang, Y.; Schulz, D.; Steiner, C. A. Physical gelation of hydrophobically modified polyelectrolytes. 1. Homogeneous gelation of alkylated poly[acrylamide-co-sodium acrylate]. *Langmuir* **1999**, *15* (13), 4335−4343.

(17) Noda, T.; Hashidzume, A.; Morishima, Y. Effects of spacer length on the side-chain micellization in random copolymers of sodium 2-(acrylamido)-2-methylpropanesulfonate and methacrylates substituted with ethylene oxide-based surfactant moieties. *Macromolecules* **2001**, *34* (5), 1308−1317.

(18) Di Cola, E.; Plucktaveesak, N.; Waigh, T. A.; Colby, R. H.; Tan, J. S.; Pyckhout-Hintzen, W.; Heenan, R. K. Structure and dynamics in aqueous solutions of amphiphilic sodium maleate-containing alternating copolymers. *Macromolecules* **2004**, *37* (22), 8457−8465.

(19) Tribet, C.; Audebert, R.; Popot, J.-L. Amphipols: Polymers that keep membrane proteins soluble in aqueous solutions. *Proc. Natl. Acad. Sci. U. S. A.* **1996**, *93*, 15047−15050.

(20) Popot, J.-L.; Althoff, T.; Bagnard, D.; Banères, J.-L.; Bazzacco, P.; Billon-Denis, E.; Catoire, L. J.; Champeil, P.; Charvolin, D.; Cocco, M. J.; Crémel, G.; Dahmane, T.; de la Maza, L. M.; Ebel, C.; Gabel, F.; Giusti, F.; Gohon, Y.; Goormaghtigh, E.; Guittet, E.; Kleinschmidt, J. H.; Kühlbrandt, W.; Le Bon, C.; Martinez, K. L.; Picard, M.; Pucci, B.; Rappaport, F.; Sachs, J. N.; Tribet, C.; van Heijenoort, C.; Wien, F.; Zito, F.; Zoonens, M. Amphipols from A to Z. *Annu. Rev. Biophys.* **2011**, *40*, 379−408.

(21) Tribet, C.; Audebert, R.; Popot, J. L. Stabilization of hydrophobic colloidal dispersions in water with amphiphilic polymers: Application to integral membrane proteins. *Langmuir* **1997**, *13* (21), 5570−5576.

(22) Gohon, Y.; Giusti, F.; Prata, C.; Charvolin, D.; Timmins, P.; Ebel, C.; Tribet, C.; Popot, J. L. Well-defined nanoparticles formed by hydrophobic assembly of a short and polydisperse random terpolymer, amphipol A8-35. *Langmuir* **2006**, *22* (3), 1281−1290.

(23) Gohon, Y.; Pavlov, G.; Timmins, P.; Tribet, C.; Popot, J.-L.; Ebel, C. Partial specific volume and solvent interactions of amphipol A8-35. *Anal. Biochem.* **2004**, *334*, 318−334.
(24) Winnik, F. M.; Regismond, S. T. A. Fluorescence methods in the study of the interactions of surfactants with polymers. *Colloid Surf. A-Phys. Eng. Aspects* **1996**, *118* (1−2), 1−39.
(25) Zoonens, M.; Giusti, F.; Zito, F.; Popot, J. L. Dynamics of membrane protein/amphipol association studied by Förster resonance energy transfer: Implications for in vitro studies of amphipol-stabilized membrane proteins. *Biochemistry* **2007**, *46* (36), 10392−10404.
(26) Ma, O.; Lavertu, M.; Sun, J.; Nguyen, S.; Buschmann, M. D.; Winnik, F. M.; Hoemann, C. D. Precise derivatization of structurally distinct chitosans with rhodamine B isothiocyanate. *Carbohydr. Polym.* **2008**, *72*, 616−624.
(27) Miller, R.; Joos, P.; Fainerman, V. B. Dynamic surface and interfacial-tensions of surfactant and polymer-solutions. *Adv. Colloid Interface Sci.* **1994**, *49*, 249−302.
(28) Fainerman, V. B.; Miller, R.; Joos, P. The measurement of dynamic surface-tension by the maximum bubble pressure method. *Colloid Polym. Sci.* **1994**, *272* (6), 731−739.
(29) (a) Mishchuk, N. A.; Fainerman, V. B.; Kovalchuk, V. I.; Miller, R.; Dukhin, S. S. Studies of concentrated surfactant solutions using the maximum bubble pressure method. *Colloid Surf. A-Phys. Eng. Aspects* **2000**, *175*, 207−216. (b) Mishchuk, N. A.; Dukhin, S. S.; Fainerman, V. B.; Kovalchuk, V. I.; Miller, R. Hydrodynamic processes in dynamic bubble pressure experiments. *Colloid Surf. A-Phys. Eng. Aspects* **2001**, *192*, 157−175.
(30) Ward, A. F. H.; Tordai, L. Time-dependence of boundary tensions of solutions the role of diffusion in time-effects. *J. Chem. Phys.* **1946**, *14* (7), 453−461.
(31) Fainerman, V. B.; Makievski, A. V.; Miller, R. The analysis of dynamic surface tension of sodium alkyl sulphate solutions, based on asymptotic equations of adsorption kinetic theory. *Colloid Surf. A-Phys. Eng. Aspects* **1994**, *87*, 61−75.
(32) Christov, N.; Danov, K.; Kralchevsky, P.; Ananthapadmanaban, K.; Lips, A. Maximum bubble pressure method: Universal surface age and transport mechanism in surfactant solutions. *Langmuir* **2006**, *22*, 7528−7542.
(33) Lorenzo, M. D.; Vinagre, H. T. M.; Joseph, D. D. Adsorption of Intan-100 at the bitumen:aqueous solution interface studied by spinning drop tensiometry. *Colloid Surf. A-Phys. Eng. Aspects* **2001**, *180*, 121−130.
(34) Joseph, D. D.; Arney, M.; Ma, G. Upper and lower bounds for interfacial tension using spinning drop devices. *J. Colloid Interface Sci.* **1992**, *148* (1), 291−294.
(35) Hernandez-Baltazar, E.; Gracia-Fadrique, J. Elliptic solution to the Young−Laplace differential equation. *J. Colloid Interface Sci.* **2005**, *287* (1), 213−216.
(36) Toomey, R.; Mays, J.; Tirrell, M. The role of salt in governing the adsorption mechanisms of micelle-forming polyelectrolyte/neutral diblock copolymers. *Macromolecules* **2006**, *39*, 697−702.
(37) Millet, F.; Perrin, P.; Merlange, M.; Benattar, J.-J. Logarithmic adsorption of charged polymeric surfactants at the air−water interface. *Langmuir* **2002**, *18*, 8824−8828.
(38) Kamyshny, A.; Magdassi, S.; Relkin, P. Chemically modified human immunoglobulin G: Hydrophobicity and surface activity at air/solution interface. *J. Colloid Interface Sci.* **1999**, *212*, 74−80.
(39) Eastoe, J.; Dalton, J. S.; Rogueda, P. G. A.; Crooks, E. R.; Pitt, A. R.; Simister, E. A. Dynamic surface tensions of nonionic surfactant solutions. *J. Colloid Interface Sci.* **1997**, *188* (2), 423−430.
(40) Goebel, J. G.; Besseling, N. A. M.; Cohen-Stuart, M.; Poncet, C. Adsorption of hydrophobically modified polyacrylic acid on a hydrophobic surface: Hysteresis caused by an electrostatic adsorption barrier. *J. Colloid Interface Sci.* **1999**, *209*, 129−135.
(41) Toomey, R.; Mays, J.; Tirrell, M. The role of salt in governing the adsorption mechanisms of micelle-forming polyelectrolyte/neutral diblock copolymers. *Macromolecules* **2006**, *39* (2), 697−702.
(42) Raju, B. B.; Winnik, F. M.; Morishima, Y. A look at the thermodynamics of the association of amphiphilic polyelectrolytes in aqueous solutions: Strengths and limitations of isothermal titration calorimetry. *Langmuir* **2001**, *17* (14), 4416−4421.
(43) Lasser, H. R.; Elias, H. G. Zur Association von Seife. III. Das associationsverhalten von β-D-*n*-octylglucosid in wasser. *Koll. Zeit. Zeit. Polym.* **1972**, *250*, 58−64.
(44) Perlmutter, J. D.; Drasler, W. J.; Xie, W.; Gao, J.; Popot, J.-L.; Sachs, J. N. All-atom and coarse-grained molecular dynamics simulations of a membrane protein stabilizing polymer. *Langmuir* **2011**, *27* (17), 10523−10537.
(45) Shih, L.-B.; Mauer, D. H.; Verbrugge, C. J.; Wu, C. F.; Chang, S. L.; Chen, S. H. Small-angle neutron scattering study of micellization of ionic copolymers in aqueous solutions. The effects of side-chain length and molecular weight. *Macromolecules* **1988**, *21* (11), 3235−3240.
(46) Colby, R. H.; Plucktaveesak, N.; Bromberg, L. Critical incorporation concentration of surfactants added to micellar solutions of hydrophobically modified polyelectrolytes of the same charge. *Langmuir* **2001**, *17* (10), 2937−2941.
(47) Millet, F.; Perrin, P.; Merlange, M.; Benattar, J. J. Logarithmic adsorption of charged polymeric surfactants at the air−water interface. *Langmuir* **2002**, *18* (23), 8824−8828.
(48) Thomas, J. L.; Barton, S. W.; Tirrell, D. A. Membrane solubilization by a hydrophobic polyelectrolyte-surface-activity and membrane-binding. *Biophys. J.* **1994**, *67* (3), 1101−1106.
(49) Vial, F.; Rabhi, S.; Tribet, C. Association of octyl-modified poly(acrylic acid) onto unilamellar vesicles of lipids and kinetics of vesicle disruption. *Langmuir* **2005**, *21* (3), 853−862.
(50) O'Shaughnessy, B.; Vavylonis, D. Non-equilibrium in adsorbed polymer layers. *J. Phys.: Condens. Matter* **2005**, *17*, R63−R99.
(51) Svitova, T. F.; Wetherbee, M. J.; Radke, C. J. Dynamics of surfactant sorption at the air/water interface: Continuous-flow tensiometry. *J. Colloid Interface Sci.* **2003**, *261*, 170−179.
(52) Charvolin, D.; Perez, J.-B.; Rouvière, F.; Giusti, F.; Bazzacco, P.; Abdine, A.; Rappaport, F.; Martinez, K. L.; Popot, J.-L. The use of amphipols as universal molecular adapters to immobilize membrane proteins onto solid supports. *Proc. Natl. Acad. Sci. U. S. A.* **2009**, *106*, 405−410.

Supporting information

Well-defined critical association concentration and rapid adsorption at the air/water interface of a short amphiphilic polymer, amphipol A8-35: a study by Förster resonance energy transfer and dynamic surface tension measurements.

Fabrice Giusti[1], Jean-Luc Popot[1,], Christophe Tribet[2,*].*

I. Characterisation of the chemical structures of FAPols.

^{1}H NMR spectra of the FAPols in MeOD

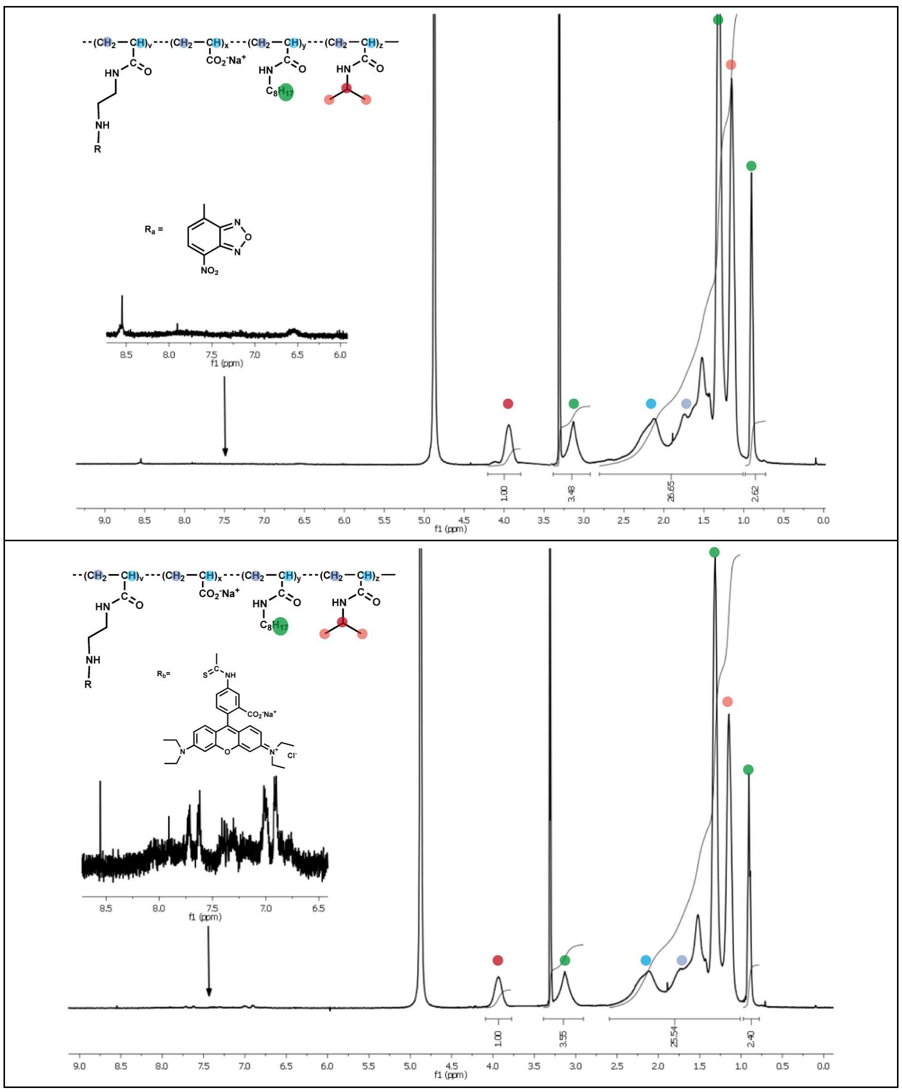

^{13}C NMR spectrum of $FAPol_{Rho}$ in D_2O.

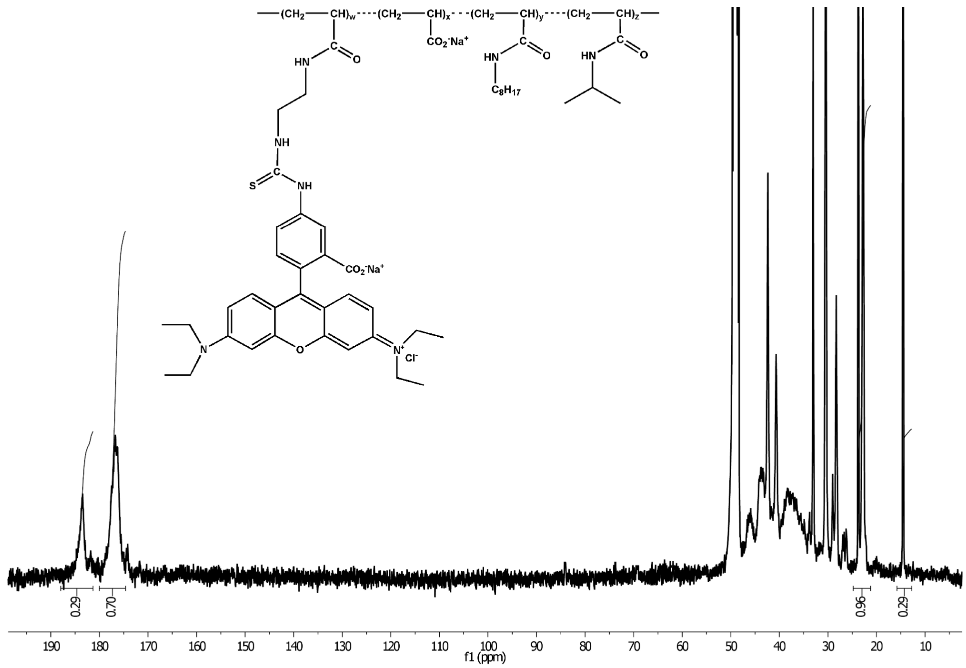

II. Estimation of the Foster distance R_0

The Förster distance between donor and acceptor molecules, R_0, at which energy transfer is 50% efficient is given by the relation (SI2):

$$R_0(\text{Å}) = 9787(K^2.\Phi_D.n^{-4}.J)^{1/6} \quad \text{(Equation SI1)}$$

with K the orientation factor assumed to be 2/3, n the refractive index of the medium[1], Φ_D the fluorescence quantum yield of the donor ($FAPol_{NBD}$) in the absence of acceptor, and J the spectral overlap integral between the emission spectrum of $FAPol_{NBD}$ and the absorption spectrum of $FAPol_{rhod}$ (see Figure 2):

$$J = \frac{10^7}{A_F}\int_0^\infty I_D(\lambda).\varepsilon_A(\lambda).\lambda^4.d\lambda \quad \text{(Equation SI2)}$$

with λ the wavelength in cm, ε_A the molar extinction coefficient of the acceptor, I_D the emission intensity of the donor, and A_F the integral over λ of the donor's emission intensities. J was calculated to be 9.50407×10^{-13} $cm^3 \cdot M^{-1}$.

Since the fluorescence quantum yield of the donor ($FAPol_{NBD}$) varies significantly with the polarity of the solvent[2], a range of R_0 values is obtained from equation SI2 depending on whether the polarity is chosen to be close to that of water or to that of apolar environments such as the globule core (see Table SI1). R_0 is close to 3.5 nm in water and reaches 6.5 nm in apolar media. The hydrodynamic radius of A8-35 particles in aqueous solution is 3.15 nm[3]. FRET is therefore expected to occur with a good efficiency between FAPol chains gathered in the same globule, as experimentally found.

Environment	NBD quantum yield	Reference	R_0 (nm) estimated in the reference cited	R_0 (nm) estimated for FAPols
water	0.015	2	-	3.5
acetone	0.49		-	6.2
DOPC bilayer	0.75	4	5.6	6.7
POPC bilayer	0.27	5	4.6	5.6
chloroform	0.60	2	-	6.4

Table SI1: Estimated values of R_0 for $FAPol_{NBD}$ and $FAPol_{rhod}$ in water and in less polar media.

III. Variation with concentration of the fluorescence intensities of FAPol solutions.

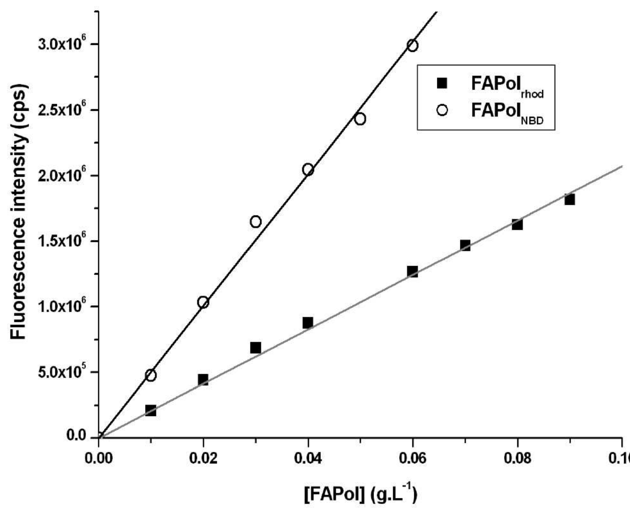

Figure SI.1: Fluorescence intensity of solutions of $FAPol_{NBD}$ (■) and $FAPol_{rhod}$ (O) in Tris buffer (pH = 8) as a function of polymer concentration. Solid lines: linear regression, with correlation coefficients R^2 = 0.9977 and R^2 = 0.9960, respectively. Excitation at 476 nm, emission measured at 575 nm.

IV. Measurement of extinction coefficient of rhodamine B in Tris buffer

In Tris buffer (NaCl 100 mM, Tris/HCl 20 mM, pH 8.0), $FAPol_{rhod}$ and free rhodamine B show comparable visible absorption spectra, as shown in Figure SI-2. The extinction coefficient of free rhodamine B was determined in this buffer from linear interpolation of measurements of the absorbance at 555 nm as a function of concentration, as shown in figure SI-3.

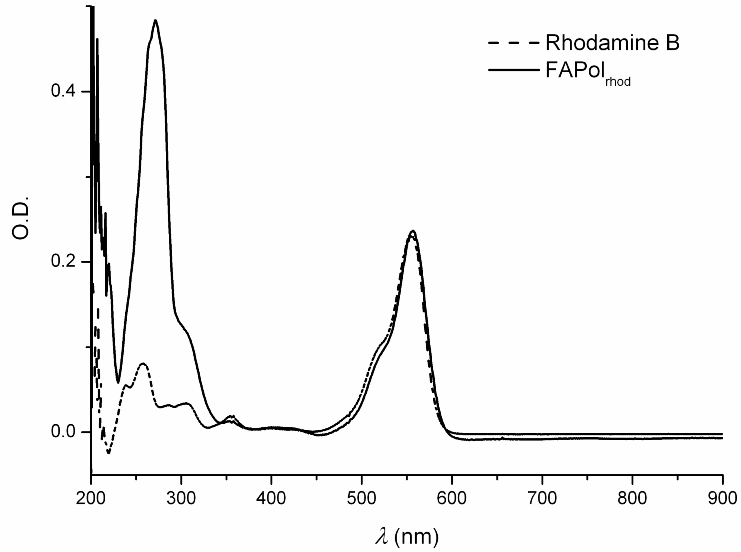

Figure SI-2: Superimposition of the absorbance spectra of 0.1 $g.L^{-1}$ $FAPol_{rhod}$ and 0.0015 $g.L^{-1}$ rhodamine B in Tris buffer.

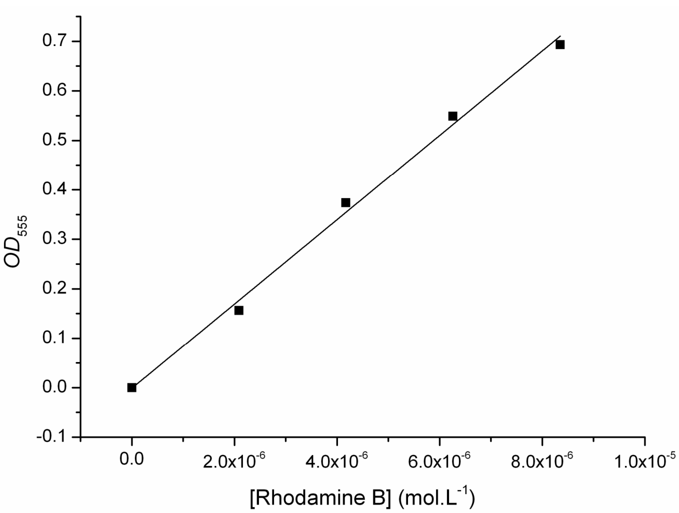

Figure SI-3. Plot of the absorbance of solutions of rhodamine B in Tris buffer and linear interpolation used to determine the molar extinction coefficient of 85,200 $cm^{-1}.mol^{-1}.L$.

References

1. M. Zoonens, F. Giusti, F. Zito, and J-L. Popot, Dynamics of Membrane Protein/Amphipol Association Studied by Förster Resonance Energy Transfer: Implications for in Vitro Studies of Amphipol-Stabilized Membrane Proteins, *Biochemistry*, **46**, 10392-10404, **2007**.
2. D. Lancet and I. Pecht, Spectroscopic and Immunochemical Studies with Nitrobenzoxadiazole alanine, a Fluorescent Dinitrophenyl Analogue?, *Biochemistry*, **16**, 5150-5157, **1977**.
3. Y. Gohon, F. Giusti, C. Prata, D. Charvolin, P. Timmins, C. Ebel, C. Tribet, J-L. Popot, *Langmuir*, Well-defined Nanoparticles Formed by Hydrophobic Assembly of a Short and Polydisperse Random Terpolymer, Amphipol A8-35, **22**, 1281-1290, **2006**.
4. J. Connor and A. J. Schroit, Determination of Lipid Asymmetry in Human Red Cells by Resonance Energy Transfer, *Biochemistry*, **26**, 5099-5105, **1987**.
5. G. Lantzsch, H. Binder, and H. Heerklotz, Surface Area per Molecule in Lipid/$C12E_n$ Membranes as Seen by Fluorescence Resonance Energy Transfer, *J. Fluorescence*, **4**, 339-343, **1994**.